6th China–Japan–Korea Joint Symposium on Optimization of Structural and Mechanical Systems
June 22-25, 2010, Kyoto, Japan

Uniqueness and Symmetry of Optimal Thickness Distribution of Axisymmetric Shells

Ryo Watada [1], Makoto Ohsaki [2] and Yoshihiro Kanno [3]

[1]Takenaka Corporation, Japan
[2]Dept. of Architecture, Hiroshima University, Higashi-Hiroshima 739-8527, Japan
ohsaki@hiroshima-u.ac.jp
[3]Dept. of Mathematical Informatics, University of Tokyo, Bunkyo, Tokyo 113-8656, Japan
kanno@mist.i.u-tokyo.ac.jp

Abstract
Uniqueness and symmetry are investigated for optimal solution of an axisymmetric shell subjected to axisymmetrically distributed loads. The compliance is minimized under constraint on the structural volume. The thickness of each element is considered as continuous design variables, and the stiffness of an element with intermediate thickness is penalized to prevent convergence to a gray solution. In contrast to the case of density variables, any solution with intermediate thicknesses is physically realizable as a solid shell structure. A solution path is defined with respect to the penalization parameter and traced using the continuation method. The rate form of the solution path is formulated from the optimality conditions, and the local non-uniqueness and symmetry breaking process of the optimal solution are rigorously investigated through the bifurcation of the solution path, where at a bifurcation point the Jacobian of the governing equations becomes singular. In the numerical examples, the symmetry-reduction process of the optimal solution as a function of the penalization parameter is studied in details. It is shown that a ribbed shell is generated through a bifurcation process of the solution path.

Keywords: Topology optimization, Uniqueness, Axisymmetric symmetry, Shell, Continuation method

1. Introduction

In most of the methods of topology optimization of continua, the 0–1 variables indicating existence/nonexistence of elements are relaxed to continuous variables between 0 and 1. However, simple solution of the relaxed problem leads to a so called gray solution, in which the variables have intermediate values between 0 and 1. In order to prevent gray solutions, two approaches called homogenization approach and density approach with penalization [1] have been developed. In the latter approach, the intermediate density is penalized to have small stiffness using, e.g., the SIMP (*solid isotropic microstructure with penalty* or *solid isotropic material with penalization*) approach [2, 3]. In the SIMP approach, a large penalization parameter results in a 0–1 solution; however, the convergence property is deteriorated if the penalization parameter is too large, because the convexity of the objective and constraint functions is lost. Therefore, the optimal solutions are traced gradually increasing the penalization parameter utilizing the so called *continuation method*.

In the predictor-corrector continuation method using the Euler predictor, the governing equations are differentiated, and the solution path is traced derivatives of the variables along the path [4]. The process of continuation is basically the same as the parametric programming approach [5, 6] or homotopy method [7] for tracing the optimal solutions corresponding to the various parameter values [8]. However, in most of the continuation methods for the plate (sheet) topology optimization problems, the governing equations are not differentiated, and the solutions are found consecutively with increasing value of the penalization parameter. Stolpe and Svanberg [9] investigated the trajectory of the optimal solutions with respect to the penalization parameter for a problem for minimizing the worst value of compliances under multiple loading conditions. Watada and Ohsaki [10] investigated local uniqueness of a path of optimal solution using a continuation method.

There have been several papers on topology optimization of symmetric plates and shells [11]. Moses *et al.* [12] investigated symmetric optimal topologies of circular plates assigning the symmetry conditions. However, to the authors' knowledge, there has been no investigation on the mechanism of symmetry-braking process of the optimal topology of axisymmetric shells. If the penalization parameter is small and intermediate density is allowed, the optimal solution of an axisymmetric shell subjected to symmetric loads is highly likely to be axisymmetric. In the same manner as bifurcation theory [13], the uniqueness of the solution is strongly related to the symmetry of the solution. Jog and Haber [14] derived the conditions of stability using incremental form of the variational problem. Petersson [15] investigated convergence of the solution with respect to the mesh size for simple loading conditions. Another difficulty in application of the SIMP approach to shells that have in-plane (membrane) and out-of-plane (bending) deformation is that a structure with intermediate density is not physically realizable.

In this study, we use thickness of each element as a design variable so that a solution with intermediate thickness can be physically manufactured or constructed as a shell with variable thickness. A small lower-bound for thickness leads to an optimal topology, whereas a moderately large lower bound leads to an optimal ribbed shell. We first define local nonuniqueness of the solution as a bifurcation of the solution path with respect to the penalization parameter. The formulation for numerical continuation with respect to the penalization parameter is rigorously derived by differentiating the Karush-Kuhn-Tucker (KKT) conditions and the stiffness (equilibrium) equations. Then, condition for local uniqueness of the solution is derived as the singularity of the Jacobian of the governing equations [13, 16, 17]. In the numerical examples, the symmetry-reduction process of the optimal solution as a function of the penalization parameter is studied in details. It is shown that a ribbed shell is generated through a bifurcation process of the solution path.

2. Optimization problem and optimality conditions

Consider a shell discretized into finite elements. The number of elements and the number of degrees of freedom are denoted by m and n, respectively. Let d_i denote the variable that defines the thickness of the ith element, for which the upper and lower bounds are assigned as

$$0 \leq d_i \leq 1, \quad (i = 1, \dots, m) \tag{1}$$

The design variable vector is given as $\boldsymbol{d} = (d_1, \dots, d_m)^\top$.

Let h_i^{U} and h_i^{L} denote the upper and lower bounds for the thickness $h_i(d_i)$ of the ith element, which is defined as

$$h_i(d_i) = h_i^{\mathrm{L}} + d_i(h_i^{\mathrm{U}} - h_i^{\mathrm{L}}) \tag{2}$$

For the thickness $\widehat{h_i}(d_i)$ for computing the stiffness, its intermediate value is penalized using a parameter p (> 0) as

$$\widehat{h_i}(d_i) = h_i^{\mathrm{L}} + d_i^p(h_i^{\mathrm{U}} - h_i^{\mathrm{L}}) \tag{3}$$

Let $\boldsymbol{F}(\boldsymbol{d}) \in \mathbb{R}^n$ denote the nodal load vector including the self-weight that is a function of $\boldsymbol{d}$. The stiffness matrix is denoted by $\boldsymbol{K}(\boldsymbol{d}) \in \mathbb{R}^{n\times n}$. Then the nodal displacement vector $\boldsymbol{U}(\boldsymbol{d}) \in \mathbb{R}^n$ is obtained from the following stiffness (equilibrium) equation:

$$\boldsymbol{K}(\boldsymbol{d})\boldsymbol{U}(\boldsymbol{d}) = \boldsymbol{F}(\boldsymbol{d}) \tag{4}$$

The objective function to be minimized is the compliance $W(\boldsymbol{d})$ defined as

$$W(\boldsymbol{d}) = \boldsymbol{F}^\top \boldsymbol{U}(\boldsymbol{d}) \tag{5}$$

The stiffness matrix $\boldsymbol{K}(\boldsymbol{d})$ is defined as follows with the matrix $\widehat{\boldsymbol{K}}_i(\widehat{h_i}) \in \mathbb{R}^{n\times n}$ of the ith element, which is also conceived as a function of d_i and written as $\boldsymbol{K}_i(d_i) \in \mathbb{R}^{n\times n}$:

$$\begin{aligned} \boldsymbol{K} &= \sum_{i=1}^{m} \widehat{\boldsymbol{K}}_i(\widehat{h_i}) \\ &= \sum_{i=1}^{m} \boldsymbol{K}_i(d_i) \end{aligned} \tag{6}$$

The volume of the ith element is expressed as a product of the area A_i and thickness h_i. Then the problem of minimizing the compliance under constraint on total structural volume is formulated with respect to the variable vector $\boldsymbol{d}$ as

$$\text{minimize} \quad W(\boldsymbol{d}) = \boldsymbol{F}^\top \boldsymbol{U}(\boldsymbol{d}) \tag{7a}$$

$$\text{subject to} \quad H(\boldsymbol{d}) = \sum_{i=1}^{m} A_i h_i - \overline{V} \leq 0 \tag{7b}$$

$$0 \leq d_i \leq 1, \quad (i = 1, \dots, m) \tag{7c}$$

where $\overline{V}$ is the specified upper bound of the total structural volume.

The Lagrangian of problem (7) is formulated as

$$L(\boldsymbol{d}, \lambda, \boldsymbol{\mu}^{\mathrm{U}}, \boldsymbol{\mu}^{\mathrm{L}}) = W(\boldsymbol{d}) + \lambda H(\boldsymbol{d}) + \sum_{i=1}^{m} \mu_i^{\mathrm{U}}(d_i - 1) + \sum_{i=1}^{m} \mu_i^{\mathrm{L}}(-d_i) \tag{8}$$

where λ, $\boldsymbol{\mu}^{\mathrm{U}} = (\mu_1^{\mathrm{U}}, \dots, \mu_m^{\mathrm{U}})$, and $\boldsymbol{\mu}^{\mathrm{L}} = (\mu_1^{\mathrm{L}}, \dots, \mu_m^{\mathrm{L}})$ are the Lagrange multipliers that have nonnegative values at the optimal solution. By differentiating Eq. (8) with respect to d_i and using Eqs. (4)–(6), we have

$$\frac{\partial L}{\partial d_i} = 2\boldsymbol{U}^\top \frac{\partial \boldsymbol{F}}{\partial d_i} - \boldsymbol{U}^\top \frac{\partial \boldsymbol{K}_i}{\partial d_i}\boldsymbol{U} + \lambda \frac{\partial H}{\partial d_i} + \mu_i^{\mathrm{U}} - \mu_i^{\mathrm{L}} \tag{9}$$

where the standard approach of sensitivity analysis of compliance has been used [18]. Define $G_i(\boldsymbol{d})$ as

$$G_i(\boldsymbol{d}) = 2\boldsymbol{U}^\top \frac{\partial \boldsymbol{F}}{\partial d_i} - \boldsymbol{U}^\top \frac{\partial \boldsymbol{K}_i}{\partial d_i}\boldsymbol{U} + \lambda \frac{\partial H}{\partial d_i} \tag{10}$$

Then the optimality conditions (KKT conditions) are derived as

$$G_i(\boldsymbol{d}) \begin{cases} = 0 & \text{for} \quad 0 < d_i < 1 \\ \leq 0 & \text{for} \quad d_i = 1 \\ \geq 0 & \text{for} \quad d_i = 0 \end{cases} \tag{11}$$

The indices of elements satisfying $0 < d_i < 1$, and, hence, $G_i(\boldsymbol{d}) = 0$, is denoted by $\mathcal{I}$; i.e.,

$$\mathcal{I} = \{i \,|\, 0 < d_i < 1\} \tag{12}$$

and the number of such elements is denoted by s.

3. Sensitivity of optimal solution with respect to penalization parameter

Equations for computing the sensitivity coefficients of the optimal solutions with respect to p, which are called parametric sensitivity coefficients for brevity, are derived below, where $(\,\cdot\,)'$ indicates differentiation with respect to p. For this purpose, the vector of state variables $\boldsymbol{U}$ and the Lagrange multiplier λ are also regarded as functions of p.

By differentiating Eq. (4) with respect to p, we have

$$-\boldsymbol{K}\boldsymbol{U}' - \left(\frac{\partial \widehat{\boldsymbol{K}}_i}{\partial \widehat{h}_i}\widehat{h}_i{}'\right)\boldsymbol{U} + \boldsymbol{F}' = \boldsymbol{0} \tag{13}$$

where $\widehat{h}_i{}'$ is obtained from Eq. (3) as

$$\widehat{h}_i{}' = (p d_i^{p-1} d_i{}' + d_i^p \ln d_i)(h_i^{\mathrm{U}} - h_i^{\mathrm{L}}) \tag{14}$$

By differentiating the volume constraint (7b), using Eq. (2), and multiplying $1/2$, we obtain

$$\frac{1}{2}\sum_{i=1}^{m} A_i (h_i^{\mathrm{U}} - h_i^{\mathrm{L}}) d_i{}' = 0 \tag{15}$$

Suppose the active side constraints remain active at the optimal solution corresponding to the parameter value in the neighborhood of the current value; i.e., $\mu_i^{\mathrm{U}} > 0$ and $\mu_i^{\mathrm{L}} > 0$ are satisfied for $d_i = 1$ and $d_i = 0$, respectively. Furthermore, transition of an inactive side constraint to being active is not considered. Hence, for the elements $i \in \mathcal{I}$, differentiation of $G_i(\boldsymbol{d}) = 0$ with respect to p leads to

$$G_i{}' = 2\boldsymbol{U}'^\top \frac{\partial \boldsymbol{F}}{\partial d_i} + 2\boldsymbol{U}^\top \left(\frac{\partial \boldsymbol{F}}{\partial d_i}\right)' - 2\boldsymbol{U}'^\top \frac{\partial \boldsymbol{K}_i}{\partial d_i}\boldsymbol{U} - \boldsymbol{U}^\top \left(\frac{\partial \boldsymbol{K}_i}{\partial d_i}\right)' \boldsymbol{U} + \lambda' \frac{\partial H(\boldsymbol{d})}{\partial d_i} + \lambda \left(\frac{\partial H(\boldsymbol{d})}{\partial d_i}\right)', \quad (i \in \mathcal{I}) \tag{16}$$

For $i \notin \mathcal{I}$, we have $d_i{}' = 0$. Therefore, there are $n + s + 1$ linear equations (13), (15), and (16) for $n + s + 1$ variables $\boldsymbol{U}'$, $d_i{}'$ $(i \in \mathcal{I})$, and λ'.

The element indices are rearranged so that $\mathcal{I} = \{1, \ldots, s\}$, and define $\boldsymbol{d}_0 = (d_1, \ldots, d_s)^\top$. Then the linear equations for computing the parametric sensitivity coefficients of the optimal solution are written in the following form using the notations defined below:

$$\begin{pmatrix} -\boldsymbol{K} & \boldsymbol{B}^{12} & \boldsymbol{0} \\ \boldsymbol{B}^{12\top} & \boldsymbol{B}^{22} & \boldsymbol{B}^{23} \\ \boldsymbol{0}^\top & \boldsymbol{B}^{23\top} & 0 \end{pmatrix} \begin{pmatrix} \boldsymbol{U}' \\ \boldsymbol{d}_0{}' \\ \lambda' \end{pmatrix} = \begin{pmatrix} \boldsymbol{b}^1 \\ \boldsymbol{b}^2 \\ 0 \end{pmatrix} \tag{17}$$

with vectors $\boldsymbol{b}_1 \in \mathbb{R}^n$, $\boldsymbol{b}_2 \in \mathbb{R}^s$, and matrices $\boldsymbol{B}^{12} \in \mathbb{R}^{n \times s}$, $\boldsymbol{B}^{22} \in \mathbb{R}^{s \times s}$, and $\boldsymbol{B}^{23} \in \mathbb{R}^s$. Eq. (17) is simply written as

$$\boldsymbol{B}\boldsymbol{X}' = \boldsymbol{b} \tag{18}$$

The path of the optimal solutions can be traced successively solving Eq. (18) [19]. Since $\boldsymbol{B}$ is symmetric, the stability of solution is detected from the eigenvalues or the condition number of the coefficient matrix in Eq. (17).

We can solve the first equation of Eq. (17) for $\boldsymbol{U}'$ as

$$\boldsymbol{U}' = -\boldsymbol{K}^{-1}\boldsymbol{b}^1 + \boldsymbol{K}^{-1}\boldsymbol{B}^{12}\boldsymbol{d}_0{}' \tag{19}$$

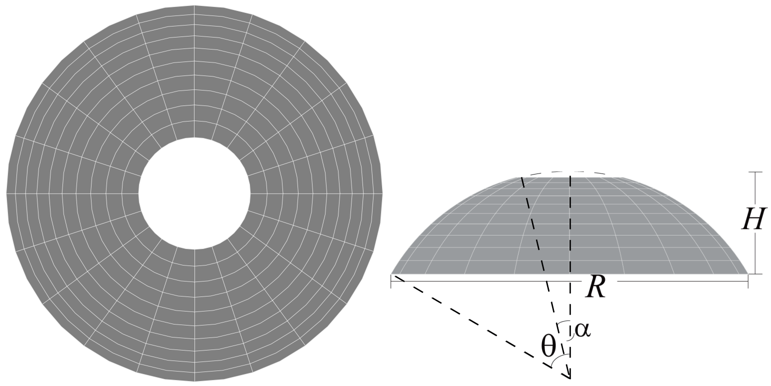

Figure 1: A spherical shell model.

which is incorporated into the second and third equations of (17) to obtain

$$\begin{pmatrix} \boldsymbol{B}^{22*} & \boldsymbol{B}^{23} \\ \boldsymbol{B}^{23\top} & 0 \end{pmatrix} \begin{pmatrix} \boldsymbol{d}'_0 \\ \lambda' \end{pmatrix} = \begin{pmatrix} \boldsymbol{b}^{2*} \\ 0 \end{pmatrix} \tag{20}$$

$$\begin{aligned} \boldsymbol{b}^{2*} &= \boldsymbol{b}^2 + \boldsymbol{B}^{12\top} \boldsymbol{K}^{-1} \boldsymbol{b}^1, \\ \boldsymbol{B}^{22*} &= \boldsymbol{B}^{22} + \boldsymbol{B}^{12\top} \boldsymbol{K}^{-1} \boldsymbol{B}^{12} \end{aligned} \tag{21}$$

Suppose there exists a singular point where the lowest eigenvalue of $\boldsymbol{B}^{22*}$ vanishes. The rate form (20) is converted to an incremental form as follows for the increments $\delta \boldsymbol{d}_0$ and $\delta\lambda$ of $\boldsymbol{d}_0$ and λ, respectively, corresponding to the increment δp of the parameter:

$$\begin{pmatrix} \boldsymbol{B}^{22*} & \boldsymbol{B}^{23} \\ \boldsymbol{B}^{23\top} & 0 \end{pmatrix} \begin{pmatrix} \delta\boldsymbol{d}_0 \\ \delta\lambda \end{pmatrix} = \delta p \begin{pmatrix} \boldsymbol{b}^{2*} \\ 0 \end{pmatrix} \tag{22}$$

Although the details are omitted, it is easily seen from Eq. (22) that bifurcation of solution occurs when $\boldsymbol{B}^{22*}$ becomes singular.

4. Numerical examples

As a numerical example, uniqueness and symmetry of optimal solution is investigated for an axisymmetric shell. The symmetry of the solution is indicated using the Schönflies notation of group theory. If the solution is invariant with respect to n different rotation operations, then it has the cyclic symmetry C_n. If the solution is invariant with respect to n different reflection operations in addition to n different rotation operations, then it has the dihedral symmetry C_{nv}.

Consider a spherical shell as shown in Fig. 1 subjected to the vertical concentrated load P at each node on the top ring. The design domain is discretized to $20 \times 10 = 200$ elements. The geometrical parameters are $R = 40.0$ m, $H = 11.5$ m, $\theta = \pi/3$, and $\alpha = \pi/12$. Young's modulus is 2.35×10^7 kN/m^2, Poisson's ratio is 0.2, and the weight density is 77.0 kN/m^3. The upper and lower bounds for the thickness are $h^{\mathrm{U}} = 0.5$ m and $h^{\mathrm{L}} = 0.1$ m, respectively. The upper-bound volume $\overline{V}$ is equal to the value corresponding to $d_i = 0.25$ for all elements. Optimization is carried out using SNOPT Ver. 7 [20], where the sequential quadratic programming (SQP) is used. The default values are used for the parameters except the strict tolerance 10^{-12} for feasibility and optimality of the solution. In the following, the units of length and force are m and kN, respectively, which are omitted for brevity.

Optimal solutions are found for the parameters between $p = 0.20$ and 2.5 with the increment $\Delta p = 0.01$, by tracing the solution path assigning the solution of $p - \Delta p$ as the initial solution for the SQP algorithm. Optimal values of $\boldsymbol{d}$ for different parameter values are shown in Fig. 2. The distributions of design variable and thickness for $p = 2.50$ are shown in Fig. 3, where h_i is normalized by h_i^{U}. The eigenvalues of $\boldsymbol{B}$ are plotted in Fig. 4 with respect to p. It is seen from Figs. 2 and 3 that ribs are clearly distributed by increasing the parameter.

The solutions with C_{20v}-symmetry are found for and all eigenvalues of $\boldsymbol{B}$ are positive for $0.20 < p < 0.63$. The lowest eigenvalues of $\boldsymbol{B}$ becomes zero in the interval $0.62 < p < 0.63$, i.e., a bifurcation point has been reached. The solution at $p = 0.63$ has C_{10v}-symetry as shown in Fig. 2. Note that the increment of $\boldsymbol{d}$ from $p = 0.62$ to 0.63 is proportional to the eigenmode as shown in Fig. 5 corresponding to the zero eigenvalue. The lowest eigenvalue vanishes also at $1.12 < p < 1.13$, where the eigenmode is as shown in Fig. 5. This way, the symmetry of solution is reduced by half through bifurcation of solution path at each bifurcation point.

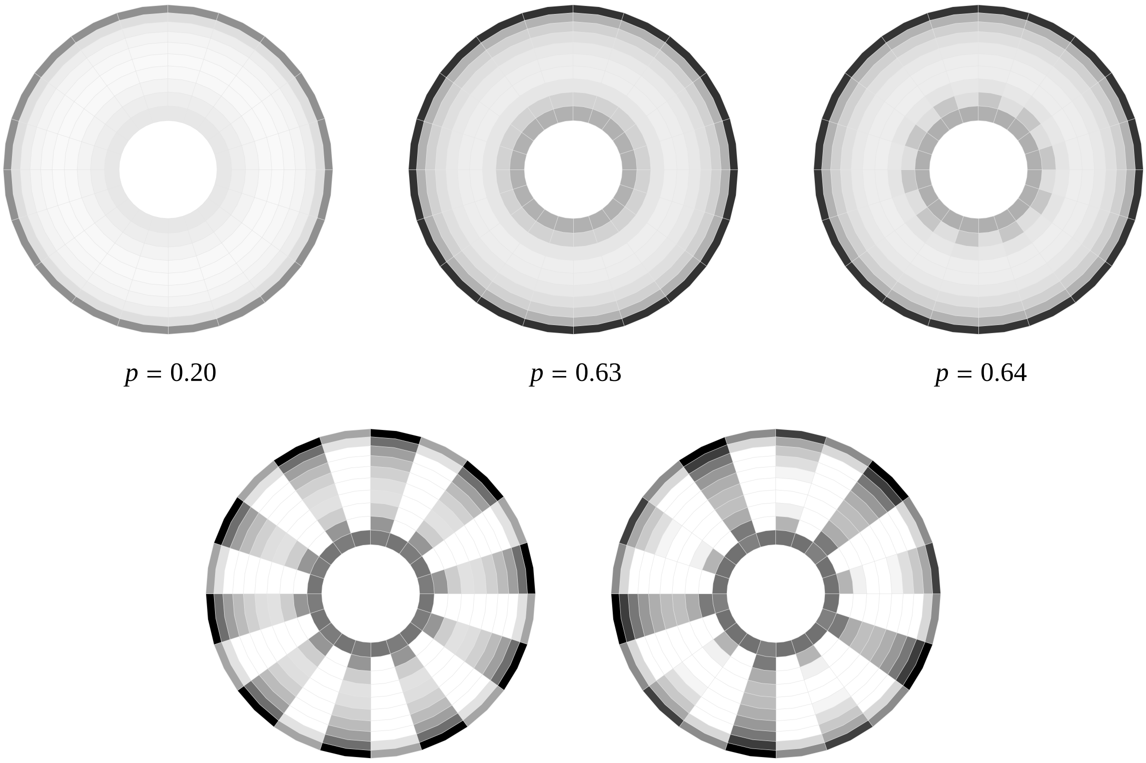

p = 0.20 p = 0.63 p = 0.64

p = 1.12 p = 1.13

Figure 2: Optimal distributions of $\boldsymbol{d}$ for various values of p.

6. Conclusions

A simple formulation has been presented for investigating the path of the optimal solution of an axisymmetric shell that minimizes the compliance under specified load and the total structural volume. A condition for nonuniqueness of the solution is derived based on a bifurcation of the solution path with respect to the penalization parameter of the SIMP approach. The formulation for a numerical continuation with the Euler predictor with respect to the penalization parameter is rigorously derived by differentiating the KKT conditions and the stiffness (equilibrium) equations, and volume constraint.

The thickness of each element, instead of its density, is taken as the design variable. Therefore, a solution with intermediate thickness can be physically constructed as a shell with variable thickness. The numerical example shows

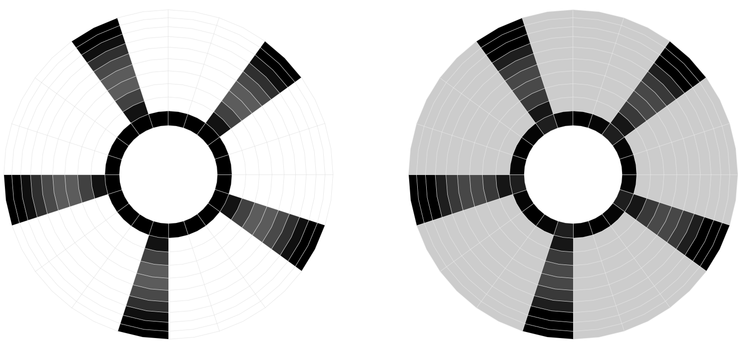

$\boldsymbol{d}$ $\boldsymbol{h}$

Figure 3: Distributions of $\boldsymbol{d}$ and $\boldsymbol{h}$ at p = 2.50.

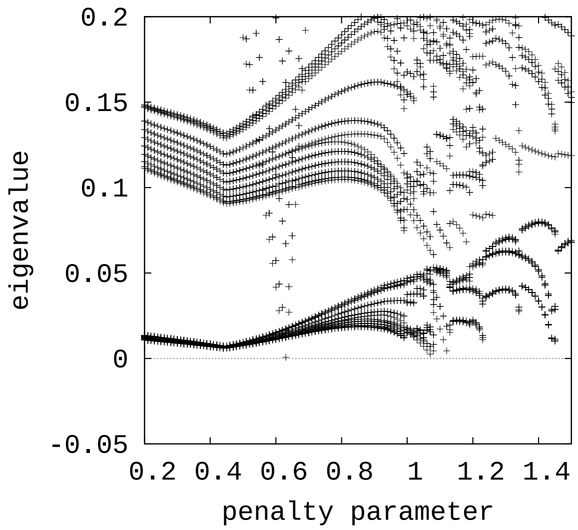

Figure 4: Eigenvalues of matrix $\boldsymbol{B}$.

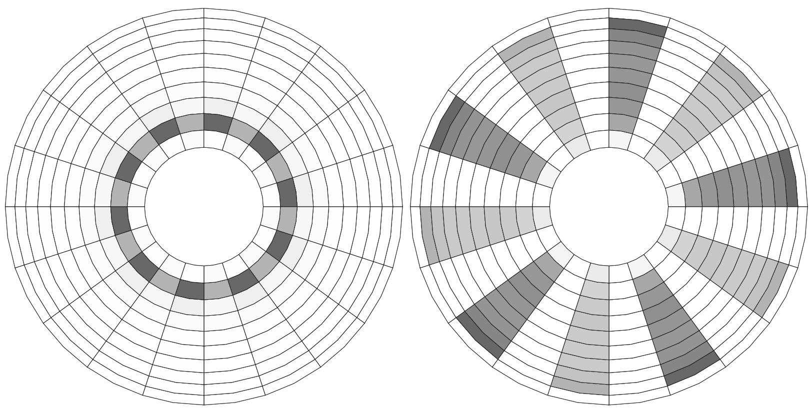

$p = 0.63$ $p = 1.12$

Figure 5: Critical eigenvector at the bifurcation point.

that the solution path of an axisymmetric shell has a bifurcation point where the Jacobian of the governing equations is singular. The optimal solution is not unique at the bifurcation point, and a symmetry-breaking bifurcation path exists in the direction of the eigenvector corresponding to the zero eigenvalue analyses of the Jacobian. This way, the symmetry-reduction process of the optimal solution is characterized as a bifurcation process of the solution path with respect to the penalization parameter. It has also been shown that a ribbed shell can be successfully generated by assigning moderately large lower-bound for thickness.

References

[1] M. P. Bendsøe. Optimal shape design as a material distribution problem. *Structural Optimization*, 1:193–202, 1989.

[2] G. I. N. Rozvany, M. Zhou, and T. Birker. Generalized shape optimization without homogenization. *Struct. Optim.*, 4:250–252, 1992.

[3] M. P. Bendsøe and O. Sigmund. *Topology Optimization: Theory, Methods and Applications*. Springer, Berlin, 2003.

[4] H. D. Mittelmann and D. Roose, editors. *Continuation Techniques and Bifurcation Problems*. Birkhäuser Verlag, Basel, Germany, 1990.

[5] T. Gal. *Postoptimal Analyses, Parametric Programming, and Related Topics*. Mc-Graw Hill, 1979.

[6] A. V. Fiacco. *Introduction to Sensitivity and Stability Analysis in Nonlinear Programming*. Academic press, 1983.

[7] L. T. Watson and R. T. Haftka. Modern homotopy methods in optimization. *Comp. Meth. Appl. Mech. Engng.*, 74(3):289–305, 1989.

[8] T. Nakamura and M. Ohsaki. Sequential optimal truss generator for frequency ranges. *Comp. Meth. Appl. Mech. Engng.*, 67(2):189–209, 1988.

[9] M. Stolpe and K. Svanberg. On the trajectories of the epsilon-relaxation approach for stress-constrained truss topology optimization. *Struct. Multidisc. Optim.*, 21:140–151, 2001.

[10] R. Watada and M. Ohsaki. Continuation approach for investigation of non-uniqueness of optimal topology for minimum compliance. In *Proc. 8th World Congress of Structural and Multidisciplinary Optimization (WCSMO8)*, number Paper No. 1073, Lisbon, 2009.

[11] F. Belblidia and S. Bulman. A hybrid topology optimization algorithm for static and vibrating shell structures. *Int. J. Num. Meth. Engng.*, 24:835–852, 2002.

[12] E. Moses, M. B. Fuchs, and M. Ryvkin. Topology design of modular structures under arbitrary loading. *Struct. Multidisc. Optim.*, 24:407–417, 2003.

[13] K. Ikeda and K. Murota. *Imperfect Bifurcation Phenomena in Structures and Materials – An Engineering Use of Group-theoretic Bifurcation Theory*. Appl. Math. Sci. Ser. 149. Springer, New York, 2002.

[14] C. S. Jog and R. B. Haber. Stability of finite element models for distributed-parameter optimization and topology design. *Comp. Meth. Appl. Mech. Engng.*, 130:203–226, 1996.

[15] J. Petersson. A finite element analysis of optimal variable thickness sheets. *SIAM J. Mumer. Anal.*, 36(6):1759–1778, 1999.

[16] M. Ohsaki. Local and global searches of approximate optimal designs of regular frames. *Int. J. Num. Meth. Engng.*, 67:132–147, 2006.

[17] M. Ohsaki and K. Ikeda. *Stability and Optimization of Structures – Generalized Sensitivity Analysis*. Springer, New York, 2007.

[18] K. K. Choi and N-H. Kim. *Structural sensitivity Analysis and Optimization 1, Linear Systems*. Springer, New York, 2004.

[19] M. Ohsaki and T. Nakamura. Minimum constraint perturbation method for topology optimization of systems. *Eng. Opt.*, 26:171–186, 1996.

[20] P. E. Gill, W. Murray, and M. A. Saunders. SNOPT: An SQP algorithm for large-scale constrained optimization. *SIAM Journal on Optimization*, 12:979–1006, 2002.